

Effect of Metal Implant Surface Topography on Fibroblast Behaviour and Bacterial Adhesion

DO.Meredith¹, L.G Harris¹, MO.Riehle², ASG.Curtis², RG.Richards¹

¹AO Research Institute, AO Foundation, Davos, CH. ²Centre for Cell Engineering, University of Glasgow, Scotland, GB.

INTRODUCTION: Internal fracture fixation implant surface finishes vary from electropolishing of stainless steel (SS) to micro-rough commercially pure titanium (cpTi) and Ti-6%Al-7%Nb (TAN). Material comparisons are difficult as the surface finish of the materials vary considerably. 'Standard' SS has a smooth 'mirror like' finish while standard cpTi and TAN are microroughened for enhanced osseointegration. This *in vitro* investigation utilised the standard material finishes and electropolished variants of cpTi and TAN. These aided in distinguishing between both material, surface chemistry and topography effects upon fibroblast growth, cytoskeletal behaviour and adhesion. Roughened SS was not included as its reduced corrosion resistance rendered it biologically and commercially non-viable. Fibroblasts are the major cellular constituent of fibrous connective tissue adjacent to implants, therefore our *in vitro* model of soft tissue interaction used human fibroblast cell line (hTERT-BJ1). Modifying the actual metal implant surface to inhibit or reduce initial bacterial adhesion may have simultaneous benefits. Therefore visualisation and quantification of *S. aureus* bacterial adhesion to standard and electropolished finishes was also performed.

METHODS: The materials tested were standard and electropolished surfaces of titanium (ISO5832/2) and Ti-6Al-7Nb (ISO 5832/11) and electropolished stainless steel (SS) (ISO 5832/1). Surface characterisation was performed using Atomic Force Microscopy (AFM), Profilometry, Scanning Electron Microscopy (SEM) and X-ray Photoelectron Spectroscopy (XPS). Qualitative cell reactivity assessment utilised SEM for cell growth and morphology at 24h, 5 and 10d timepoints. Intracellular components, vinculin, tubulin, actin and DNA, were fluorescently labelled and imaged using the Fluorescence Microscope (FM) at 48h. DNA from cells cultured for 24h, 5 and 10d was extracted and quantified to confirm qualitative cell growth findings.

To visualise bacterial adherence, *S. aureus* were cultured on the different surfaces in a brain heart infusion broth at 37°C for 1 hour, then fixed for

SEM imaging. To quantify the amount of adherent bacteria, they were stained with fluorescent 5-cyano,2-ditoyl tetrazolium chloride (CTC), and visualized with FM. The density of live bacteria on the surfaces in each image were counted using KS400 software and analysed statistically using a one-way ANOVA with Tukey test. This was repeated three times. Statistical significance was accepted at $p \leq 0.05$.

RESULTS: SS, TE and NE were all smooth samples with Ra's between 0.18-0.19 μ m (Table 1). While similar in Ra, AFM (Fig 1a) and SEM demonstrated that all materials had some variation in topographical morphology. SS had some surface scratches, TE had a topography of nanometric surface nodules and NE displayed an undulating topography. The rougher materials, TS and NS had higher but similar Ra's of 0.90 and 0.77 μ m. AFM and SEM demonstrated that the similarities end here with TS having a rugged irregular surface, NS demonstrating a 'microspiked' topography consisting of protruding particles. XPS showed that electropolishing the cpTi or TAN followed by anodisation did not add any contamination to the final surface chemistry (table 2).

Surface	code	Ra (μ m)
Std micro-rough titanium	TS	0.90 \pm 0.027
Electropolished TS	TE	0.19 \pm 0.030
Std micro-rough Ti-6Al-7Nb	NS	0.77 \pm 0.076
Electropolished NS	NE	0.18 \pm 0.037
Std electropolished stainless steel	SS	0.19 \pm 0.022

Table 1. Surface Roughness Parameter Ra for the different surfaces.

	Atomic Concentration [%]								
	Al 2p	C 1s	N 1s	Na KLL	Nb 3d	O 1s	P 2p	Ti 2p	
NS	1.7	25.5	0.9	0.8	0.2	51.2	2.1	17.6	
NE	2.0	27.8	1.1	0.4	0.1	49.3	0.6	18.6	
TS	n/a	26.95	0.6	1.2	n/a	50.7	3.0	17.5	
TE	n/a	32.1	1.3	0.3	n/a	47.0	2.6	16.4	
	Cr 2p	C 1s	Fe 2p	N 1s	Mo 3d	Na 1s	O 1s	P 2p	Ni 2p
SS	7.3	41.4	4.5	3.7	0.6	1.5	40.1	0.3	0.8

Table 2. XPS surface chemical analysis of the various surfaces (n/a – not applicable).

Qualitative cell growth on the samples, by SEM, demonstrates that cells reached confluency by the 10d timepoint on all samples except NS. This growth suppression was confirmed to a level of statistical significance ($P > 0.01$) by DNA quantification. Cell morphologies were well spread on SS, TE and NE at both 24h and 5d timepoints. The morphology only changed due to lack of surface space, and cells adopted an elongated morphology. Cells on TS were not well spread at 24h with investigatory filopodia emanating from far within the cell body. By 5d, cells were better spread and 10d were elongated with confluent numbers. On NS, cells at all timepoints were rounded or elongated. At 24h and 5d filopodia could be seen attaching to the microspikes, however by 10d this exploration had ceased. On some cells, membrane integrity was reduced to a much coarser texture indicative of cell necrosis. Intracellular labelling demonstrated that on SS, TE and NE the focal adhesion (FA) sites were mature with associated actin cytoskeleton and a well conserved microtubule network. On TS, cells were less spread with smaller FA but a well-conserved actin and microtubule network. For NS (Fig 1b), cells were again unspread and FA's were small and could be observed avoiding the microspikes. The underlying microspikes could also be seen actively impairing for formation of the microtubule network.

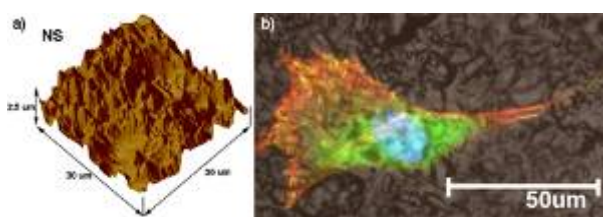


Fig1(a) AFM of NS. (b) Fluorescence microscopy of the cell cytoskeleton and adhesion sites on NS.

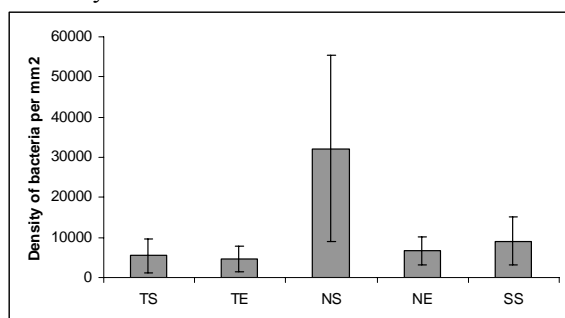


Fig 3. Graph showing the average density of living *S. aureus* adhering to the different surfaces (n=3cultures).

The large variations are due to clumping of the bacteria on the surface.

Qualitative and quantitative results of *S. aureus* adhesion on the different surfaces correlated with each other, and showed significantly more live bacteria on NS than on the other surfaces, whilst there was no significant difference between the amount of bacteria on TS, TE, NE and SS surfaces (Fig 3). The results showed a significant decrease in the amount of bacteria adhering to the NE compared to standard NS surfaces.

DISCUSSION & CONCLUSIONS: Our findings indicate that surface chemistry is not paramount to cytocompatibility. NE's bio-performance (with regards to fibroblasts) was exceptional in comparison with its microrough counterpart, NS. A general roughened topography was also not the cause as both TE and its roughened counterpart, TS, performed well. As can be seen from the interaction of the filopodia, FA's and microtubules, the additional factor of NS is its unique microspiked topography, an inherent characteristic of the TAN microstructure. They are also present in a smoothed rounded edged form in NE, but are of no significance to subsequent cytocompatibility studies. Thus we propose that the topographical presence and dimensions of the particles present on NS inhibits the spreading of cells and development of mature FA's; two essential factors in the progression of the cell cycle and cell growth.

With regards to bacterial adhesion, this study found that electropolishing Ti-6Al-7Nb surfaces (NE) significantly decreased the amount of *S. aureus* adhesion compared to the standard Ti-6Al-7Nb (NS), which had a higher affinity to the bacteria than the other surfaces tested. This would indicate that the aforementioned microspikes of NS increase *S. aureus* adhesion and could lead to higher infection rates *in vivo*. Hence electropolishing Ti-6Al-7Nb surfaces could be advantageous in osteosynthesis areas as a measure to prevent soft-tissue irritation while also minimising bacterial adhesion, possibly even lowering the rate of infection. *In vivo* tests will have to be carried out to confirm this interesting development.

Acknowledgments: Thanks to Robert Mathys Foundation (RMS), Switzerland for the surfaces, and to Dr Vinzenz Frauchiger (RMS) for the XPS analysis of the surfaces.